J. Plasma Physics (2010), *vol.* 76, *part* 2, *pp.* 135–158. © Cambridge University Press 2009
doi:10.1017/S0022377809990031

Solar coronal heating by plasma waves

R. BINGHAM[1], P.K. SHUKLA[2], B. ELIASSON[3] and L. STENFLO[3]

[1]Rutherford Appleton Laboratory, Chilton, Oxon, OX11 0QX, UK
Also at SUPA Department of Physics, University of Strathclyde, Glasgow, Scotland
(bob.bingham@stfc.ac.uk, ps@tp4.ruhr-uni-bochum.de)

[2]Institut für Theoretische Physik IV, Ruhr-Universität Bochum, D-44780 Bochum, Germany
Also at SUPA Department of Physics, University of Strathclyde, Glasgow, Scotland

[3]Department of Physics, Umeå University, SE-90187 Umeå, Sweden

(Received 16 March 2009 and accepted 6 April 2009, first published online 16 June 2009)

Abstract. The solar coronal plasma is maintained at temperatures of millions of degrees, much hotter than the photosphere, which is at a temperature of just 6000 K. In this paper, the plasma particle heating based on the kinetic theory of wave–particle interactions involving kinetic Alfvén waves and lower-hybrid drift modes is presented. The solar coronal plasma is collisionless and therefore the heating must rely on turbulent wave heating models, such as lower-hybrid drift models at reconnection sites or the kinetic Alfvén waves. These turbulent wave modes are created by a variety of instabilities driven from below. The transition region at altitudes of about 2000 km is an important boundary chromosphere, since it separates the collision-dominated photosphere/chromosphere and the collisionless corona. The collisionless plasma of the corona is ideal for supporting kinetic wave–plasma interactions. Wave–particle interactions lead to anisotropic non-Maxwellian plasma distribution functions, which may be investigated by using spectral analysis procedures being developed at the present time.

1. Introduction

A central problem in solar physics is the coronal heating mechanism which requires an input of non-thermal energy to sustain the temperature at millions of degrees, much hotter than the photosphere. The temperature continues to rise slowly throughout the chromosphere followed by a steep rise at the transition region up to 5 million K in the corona (Feldman and Landi 2008). The energy content of the coronal plasma at 1.6 J/m^3 is however substantially smaller, with an X-ray brightness of 1 W/cm^2, compared to 3 kJ/m^3 and a brightness of 6.4 kW/cm^3 for the photosphere, which radiates at a temperature of about 6000 K. Detailed measurements of the X-ray-emitting corona by past and present satellite missions such as Skylab, SMM and SOHO have contributed enormously to our knowledge of the corona. From the soft X-ray observations the corona is seen as a highly filamentary, inhomogeneous structure consisting of a complex myriad of magnetic loop-like structures, with the hottest plasmas found in regions of high magnetic field activity, which also contain the largest magnetic fields. Thousands of X-ray bright points or blinkers (Harrison 1997) are seen bubbling on the surface and

https://doi.org/10.1017/S0022377809990031 Published online by Cambridge University Press

associated with cancellation of opposing magnetic flux. In closed magnetic field structures, for example in active regions, temperatures may reach up to 10 million K while in open magnetic field regions, such as coronal holes, temperatures are about 1 million K. A number of heating mechanisms have been proposed ranging from hydrodynamic, i.e. acoustic wave, heating, magnetohydrodynamic heating to microstructures involving plasma kinetic theory. In deciding which particular model is relevant it is important to understand the plasma conditions where the heating processes are taking place. It is also important to identify the free energy available for plasma heating and how it is transported into the region. The real problem is to understand how the transported energy is dissipated efficiently. This is where an understanding of the plasma conditions is important. The energy source for heating is undoubtedly the kinetic energy of plasma flows driven by thermal convection in the photosphere, where the plasma's β ($= nkT/B^2/2\mu_0$) is of order 1 or greater, resulting in the magnetic field being advected with the plasma flows. In the highly tenuous corona with temperatures of the order of hundreds of eV and densities of 10^{10} cm^{-3}, the plasma β is 0.1–0.01, the field pressure dominates in this region and there is a strong indication that heating is correlated with intense magnetic field activity in filamentary structures. This is supported by inhomogeneities in temperature and magnetic field structures; also, the strength of the magnetic field correlates well with corona temperatures in other stars (Kellett and Tsikoudi 1997). Given the high temperature and low density, the coronal plasma is collisionless and lends itself to kinetic wave heating processes. The transition region separates the solar atmosphere into two regions: the photosphere is collision dominated, the chromosphere is also dominated by collisions between particles, electrons, ions and neutrals, while the corona is collisionless. The difference in collisionality is important in beginning to understand the difference in temperatures between the two regions. In the high-β plasma of the photosphere where the density is high and the temperature is low, collisions keep the plasma in thermal equilibrium as well as preventing rapid growth of instabilities giving rise to plasma waves. The opposite situation exists in the corona where the low-density collisionless plasma provides the ideal environment for the free-energy sources to strongly drive plasma instabilities giving rise to turbulent wave motions which rapidly heat the plasma. The plasma in this region is highly non-thermal due to the lack of collisions; non-thermal electron and ion distribution functions exist in this region. In the collisionally dominated photosphere the free energy in magnetic fields or plasma flows is not readily converted to microscopic turbulent wave motion; the dissipation is normally through Joule heating due to currents or viscosity. The free energy is rapidly thermalized by collisions, the free energy being shared by a large number of particles. In the collisionless corona the free energy finds its way relatively easily through a number of instabilities to wave turbulence. The collisionless dissipation of turbulent waves is governed by the wave–particle resonance condition $\omega - k_\parallel v_\parallel - n|\omega_{cj}| = 0$, $j =$ electron, ion; $n = 0, \pm 1, \pm 2, \ldots, \omega_{cj} = eB/m_j$ is the cyclotron resonance for species j, e is the electron charge, B is the magnetic field strength and m_j is the mass of particle j. The Landau (or Cerenkov) resonance condition arises for $n = 0$; particles moving parallel to the magnetic field exchange energy with the waves. Particles gain energy by Landau damping the waves, such as lower-hybrid waves, kinetic and compressional Alfvén waves, etc. $n = \pm 1$ corresponds to cyclotron resonance between the waves and the particles. The perpendicular velocity of the particles changes during cyclotron resonance,

https://doi.org/10.1017/S0022377809990031 Published online by Cambridge University Press

examples being either electron or ion cyclotron heating. In all cases of wave–particle interactions non-thermal anisotropic distribution functions are created. Thermalization occurs slowly through nonlinear diffusion processes. Anisotropic distribution functions or non-Maxwellian distributions are observed by satellites in the solar wind. Many mechanisms have been proposed for the solar coronal heating (Edwin and Murawski 1995; Laing and Edwin 1995; Narain and Ulmschneider 1996). These include the dissipation of ion acoustic and magnetosonic waves as well as magnetic reconnection and the filamentation instability of low-frequency Alfvén waves (Champeaux et al. 1997). Any proposed theory has to consider both the electron and ion heating mechanisms. Here, we will describe examples of possible wave heating processes, including kinetic Alfvén waves and lower-hybrid waves generated at sites of reconnections or shocks. Gradients in density, magnetic field and temperature are also important free-energy sources that can drive drift-mode turbulence. The transition region can be thought of as a free-energy source for drift modes.

2. The Alfvén waves

The Alfvén wave (Alfvén 1942) is classic in plasma physics. In the Alfvén wave, the restoring force comes from the pressure of the magnetic fields, and the ion mass provides the inertia. The propagation of low-frequency (in comparison with ω_{ci}) non-dispersive Alfvén waves is basically governed by the ideal magnetohydrodynamic (MHD) equations. The dispersion of Alfvén waves arises due to the finite ω/ω_{ci} and the parallel electron inertial force in a cold plasma, as well as from the finite ion Larmor radius and the parallel electron pressure gradient in a warm plasma (Brodin and Stenflo 1990; Hasegawa and Chen 1976; Hasegawa and Uberoi 1982; Shukla and Stenflo 2000a, 2004; Stefant 1971). Owing to non-ideal effects Alfvén waves also couple to other plasma modes, viz. magnetosonic waves, whistlers, etc. The dispersive Alfvén waves have wide-ranging applications in space, fusion and laboratory plasmas (Gekelman 1999; Kletzing et al. 2003; Whitlam et al. 2002). Specifically, large-amplitude Alfvén waves transport a considerable amount of energy from the distant parts of the magnetosphere to the near-Earth space, and play a significant role in the solar corona and in the solar wind. Large-amplitude Alfvén waves can cause a number of nonlinear effects (Brodin and Stenflo 1990; Diamond and Malkov 2006; Drozdenko and Morales 2001; Hasegawa and Uberoi 1982; Shukla 2005; Shukla and Dawson 1984; Shukla and Stenflo 1985, 1995, 1999a,b, 2000b, 2000c, Shukla et al. 1998, 1999). The latter include harmonic generation for non-circularly polarized waves, parametric processes such as three-wave decay interactions, stimulated Compton scattering, modulational and filamentational interactions, as well as the modification of the background plasma number density by the Alfvén wave ponderomotive force, the formation of Alfvén vortices and current filaments due to the Alfvén wave mode couplings, the generation of zonal flows by the Reynolds stress of the kinetic Alfvén waves, as well as the electron and ion heating due to wave–particle interactions. Understanding the nonlinear properties of dispersive Alfvén waves is a necessary prerequisite in interpreting the numerous observations of large-amplitude, low-frequency (in comparison with the electron gyrofrequency) dispersive electromagnetic waves in laboratory and space plasmas. We first discuss the linear properties of dispersive Alfvén waves and their relations to other modes in a uniform magnetoplasma. We

https://doi.org/10.1017/S0022377809990031 Published online by Cambridge University Press

then include arbitrary ion gyroradius and parallel phase speed effects, as well as ω/ω_{ci} corrections. The finite ion gyroradius effect in the shear Alfvén wave (both inertial Alfvén (IA) and kinetic Alfvén (KA) waves) theory can be considered by means of the kinetic ion response (Brambilla 1988), while for waves with parallel phase speed comparable to the electron thermal speed one has to resort to a gyrokinetic electron response that accounts for the wave–electron interactions. Furthermore, the IA and KA waves have to be treated separately as they have parallel phase speeds $V_p = \omega/k_z$ satisfying opposing limits (viz. $V_p \gg V_{Te}$ for the IA waves and $V_p \ll V_{Te}$ for the KA waves), where ω is the wave frequency, k_z is the magnetic field-aligned wavenumber and V_{Te} is the electron thermal speed. Second, we go on to describe the Alfvén wave ponderomotive force induced density modifications in the background plasma, as well as the localization of magnetic field-aligned circularly polarized Alfvén waves. Third, we consider the mode couplings between dispersive Alfvén waves in plasmas. Fourth, we present a theory (Shukla 2005) for the excitation of zonal flows by the Reynolds stresses of the kinetic Alfvén waves. Fifth, we provide a mechanism for heating the electrons (ions) by obliquely (magnetic field-aligned) propagating high-frequency electromagnetic ion-cyclotron-Alfvén (left-hand circularly polarized ion cyclotron) waves, due to the wave–electron (ion) resonance interaction. We demonstrate electron heating in the solar corona by the high-frequency (comparable with ω_{ci}) dispersive kinetic Alfvén waves (HFDKAWs), whose parallel wavelength is of the order of the ion skin depth $\lambda_i = c/\omega_{pi}$, where c is the speed of light, $\omega_{pi} = (4\pi n_0 e^2/m_i)^{1/2}$ the ion plasma frequency and e the magnitude of the electron charge. The HFDKAWs in the solar corona could be generated either by the supergranular network through small-scale magnetic reconnection events (McKenzie et al. 1995) or by the mode conversion (Bingham et al. 2001; Hasegawa and Chen 1976) of surface Alfvén waves at the Alfvén resonance layer where the frequency ω equals $\omega_A/(1+k_z^2\lambda_i^2)^{1/2}$. Here, $\omega_A = k_z\nu_A$ is the Alfvén wave frequency, k_z the component of the wavevector along the external magnetic field $B_0\hat{\mathbf{z}}$, $\hat{\mathbf{z}}$ being the unit vector along the z axis, and $\nu_A = B_0/(4\pi n_0 m_i)^{1/2}$ the Alfvén velocity.

3. Linear properties

Let us consider a homogeneous plasma in an external magnetic field $\hat{\mathbf{z}}B_0$, where $\hat{\mathbf{z}}$ is the unit vector along the z direction and B_0 is the strength of the magnetic field. The dynamics of Alfvén waves within the simplest model is governed by the ideal MHD equations (Shukla et al. 2004)

$$\frac{dn}{dt} + n\nabla\cdot\mathbf{u} = 0, \tag{1}$$

$$\frac{d\mathbf{u}}{dt} = \frac{(\nabla\times\mathbf{B})\times\mathbf{B}}{4\pi\rho} \tag{2}$$

and

$$\frac{\partial\mathbf{B}}{\partial t} = \nabla\times(\mathbf{u}\times\mathbf{B}), \tag{3}$$

where Ohm's law

$$\mathbf{E} + \frac{\mathbf{u}\times\mathbf{B}}{c} = 0 \tag{4}$$

https://doi.org/10.1017/S0022377809990031 Published online by Cambridge University Press

has been used. Here, $d/dt = (\partial/\partial t) + \mathbf{u}\cdot\nabla$ and $\rho = nm_{\rm i}$, where n is the ion number density, $\mathbf{u}$ is the ion fluid velocity, $\mathbf{E}$ and $\mathbf{B}$ are electric and magnetic fields, respectively, $m_{\rm i}$ is the ion mass and c is the speed of light in vacuum. The field-frozen condition (n/B = constant) follows from (1) and (3). The Alfvén wave frequency is $\omega = kV_{\rm A} \equiv kB_0/\sqrt{4\pi n m_{\rm i}}$, which shows that the restoring force comes from the magnetic pressure while the ion mass provides inertia to maintain the wave. The dispersion of the Alfvén wave comes from the generalized Ohm's law

$$\mathbf{E} + \frac{\mathbf{u}\times\mathbf{B}}{c} - \frac{\nabla\times\mathbf{B}}{4\pi en} + \frac{\nabla P_{\rm e}}{en} = 0, \tag{5}$$

which thus replaces (4), and which is valid for waves with frequencies much smaller than the electron gyrofrequency $\omega_{\rm ce} = eB_0/m_{\rm e}c$, where e is the magnitude of the electron charge and $m_{\rm e}$ is the electron mass. Equation (5) takes into account the differential motion between the electrons and ions, as well as the finite electron pressure gradient $\nabla P_{\rm e}$. Substituting (5) into the ion momentum equation and Faraday's law, we obtain

$$\frac{d\mathbf{u}}{dt} = \frac{(\nabla\times\mathbf{B})\times\mathbf{B}}{4\pi\rho} - \frac{\nabla P}{\rho} \tag{6}$$

and

$$\frac{\partial\mathbf{B}}{\partial t} = \nabla\times\left[\left(\mathbf{u} - \frac{c\nabla\times\mathbf{B}}{4\pi en}\right)\times\mathbf{B}\right], \tag{7}$$

where $P = P_{\rm e} + P_{\rm i} \equiv n(T_{\rm e} + T_{\rm i})$ is the sum of the electron and ion pressures. Equations (1), (6) and (7) are known as the nonlinear Hall-MHD equations. It turns out that the Hall velocity $\mathbf{u}_{\rm H} = -c\nabla\times\mathbf{B}/4\pi en$ in (7) introduces a new spatial scale, the ion skin depth $c/\omega_{\rm pi}$, where $\omega_{\rm pi}$ is the ion plasma frequency. It also allows us to consider phenomena that are occurring on a time scale smaller than the ion gyroperiod $\omega_{\rm ci}^{-1}$, where $\omega_{\rm ci} = eB_0/m_{\rm i}c$ is the ion gyrofrequency. The waves in our Hall-MHD plasma are governed by the dispersion relation (Brodin and Stenflo 1990; Shukla and Stenflo 1999a)

$$(\omega^2 - k_z^2V_{\rm A}^2)D_{\rm m}(\omega,\mathbf{k}) = \frac{\omega^2}{\omega_{\rm ci}^2}k_z^2k^2(\omega^2 - k^2V_{\rm s}^2)V_{\rm A}^4, \tag{8}$$

where

$$D_{\rm m}(\omega,\mathbf{k}) = \omega^4 - \omega^2k^2(V_{\rm A}^2 + V_{\rm s}^2) + k_z^2k^2V_{\rm A}^2V_{\rm s}^2 \tag{9}$$

and $V_{\rm s}$ is the effective sound speed. Equation (8) shows that the Alfvén and magnetoacoustic waves are coupled due to a finite $\omega/\omega_{\rm ci}$ effect. Equation (8) also contains the kinetic Alfvén and long-wavelength (in comparison with the electron skin depth $\lambda_{\rm e} = c/\omega_{\rm pe}$) electron whistlers. The latter usually have $\sqrt{\omega_{\rm ce}\omega_{\rm ci}} \ll \omega \ll kc \ll \omega_{\rm pe}$, where $\omega_{\rm pe}$ is the electron plasma frequency. The dynamics of nonlinear whistlers is governed by the electron-MHD (E-MHD) equation

$$\frac{D\mathscr{B}}{Dt} - \mathscr{B}\cdot\nabla\mathbf{V} = 0, \tag{10}$$

where $\mathscr{B} = \mathbf{B} - \lambda_{\rm e}^2\nabla^2\mathbf{B}$, $D/Dt = (\partial/\partial t) + \mathbf{V}\cdot\nabla$ and $\mathbf{V} = -c\nabla\times\mathbf{B}/4\pi en$ is the electron fluid velocity. The ions are assumed to be immobile. In the linear limit, (10) admits obliquely propagating whistlers whose frequency is

$$\omega = \frac{k^2c^2\omega_{\rm ce}\cos\theta}{\omega_{\rm pe}^2 + k^2c^2}, \tag{11}$$

https://doi.org/10.1017/S0022377809990031 Published online by Cambridge University Press

where $\cos\theta = k_z/k$. In the long-wavelength limit, viz. $kc \ll \omega_{pe}$, we have from (11)

$$\omega = \frac{k_z k c^2 \omega_{ce}}{\omega_{pe}^2}, \tag{12}$$

which reduces to (Shukla 1978)

$$\omega = \frac{k_z^2 c^2 \omega_{ce}}{\omega_{pe}^2} \tag{13}$$

when the perpendicular component of the wavevector is zero. Next, we discuss the properties of dispersive shear Alfvén waves (DSAWs) (Gekelman 1999), whose electric and magnetic fields are $\mathbf{E} = -\nabla\phi - c^{-1}\hat{\mathbf{z}}\partial A_z/\partial t$ and $\mathbf{B}_\perp = \nabla A_z \times \hat{\mathbf{z}}$, respectively, where ϕ is the scalar potential and A_z is the parallel (to $\hat{\mathbf{z}}$) component of the vector potential. The electron density perturbation n_{e1} associated with low-frequency (in comparison with the electron gyrofrequency) DSAWs is given by

$$n_{e1} = -\frac{k_z J_z}{\omega e}, \tag{14}$$

where the parallel (to $\hat{\mathbf{z}}$) component of the electron current density is (Shukla and Stenflo 2004)

$$J_z = -\frac{\omega n_0 e^2}{k_z^2 T_e} W(\xi)\left(\frac{\omega}{c}A_z - k_z\phi\right), \tag{15}$$

where $W(\xi) = -[1 + \xi Z(\xi)]$, $\xi = V_p/V_{Te}$, $V_{Te} = (T_e/m_e)^{1/2}$ is the electron thermal speed, T_e is the electron temperature, n_0 is the unperturbed value of n and $Z(\xi)$ is the standard plasma dispersion function. In deriving (15), we assumed that $k_\perp^2\rho_e^2 \ll 1$, where $k_\perp$ is the component of the wavevector perpendicular to $\hat{\mathbf{z}}$ and $\rho_e = V_{Te}/\omega_{ce}$ is the electron gyroradius. From the parallel component of Ampère's law, we have

$$J_z = \frac{c}{4\pi}k_\perp^2 A_z, \tag{16}$$

so that from (14)–(16) we obtain (Shukla and Stenflo 2004)

$$n_{e1} = -\frac{n_0 e}{T_e}\frac{k_\perp^2 c^2 k_z^2 \lambda_{De}^2 W(\xi)}{[k_\perp^2 c^2 k_z^2 \lambda_{De}^2 + \omega^2 W(\xi)]}\phi, \tag{17}$$

where $\lambda_{De} = (T_e/4\pi n_0 e^2)^{1/2}$ is the electron Debye radius. The expression (17) incorporates the electron Landau effect. For finite values of ω/ω_{ci} and $b_i = k_\perp^2\rho_i^2$, where $\rho_i = V_{Ti}/\omega_{ci}$ is the ion gyroradius, $V_{Ti} = (T_i/m_i)^{1/2}$ is the ion thermal speed and T_i is the ion temperature, the expression for the ion number density perturbation n_{i1} has to be obtained by integrating the ion distribution function calculated from the linearized Vlasov equation. For two-dimensional ion motions across $\hat{\mathbf{z}}$, we have (Brambilla 1988)

$$n_{i1} \simeq -n_0\left[1 - \Gamma_0(b_i) - \frac{2\Gamma_1(b_i)\omega^2}{\omega^2 - \omega_{ci}^2}\right]\frac{e\phi}{T_i}, \tag{18}$$

where $\Gamma_{0,1}(b_i) = I_{0,1}(b_i)\exp(-b_i)$ and I_0 (I_1) is the modified Bessel function of zero (first) order. Invoking the quasi-neutrality $n_{e1} = n_{i1}$, we have from (17) and (18)

$$1 - \Gamma_0(b_i) - \frac{2\Gamma_1(b_i)\omega^2}{\omega^2 - \omega_{ci}^2} - \frac{T_i}{T_e}\frac{k_\perp^2 c^2 k_z^2 \lambda_{De}^2 W(\xi)}{[k_\perp^2 c^2 k_z^2 \lambda_{De}^2 + \omega^2 W(\xi)]} = 0, \tag{19}$$

https://doi.org/10.1017/S0022377809990031 Published online by Cambridge University Press

which is the general dispersion relation for the coupled ion-cyclotron-dispersive Alfvén waves in plasmas. We now focus on the inertial Alfvén (IA) and kinetic Alfvén (KA) waves for which $\xi \gg 1$ and $\xi \ll 1$, respectively. Thus, the corresponding electron number densities, found from (17), are, respectively,

$$n_{e1}^{I} = -\frac{k_z^2 c^2 k_\perp^2}{4\pi e(1+b_e)\omega^2}\phi \tag{20}$$

and

$$n_{e1}^{K} = -\frac{k_z^2 c^2 k_\perp^2}{4\pi e(\omega^2 - k_z^2 V_A^2 b_s)}\phi, \tag{21}$$

where $b_e = k_\perp^2\lambda_e^2$, $b_s = k_\perp^2\rho_s^2$, $\lambda_e = c/\omega_{pe}$ is the electron skin depth, $\rho_s = C_s/\omega_{ci}$ is the sound gyroradius and $C_s = (T_e/m_i)^{1/2}$ is the ion sound speed. The superscripts I and K denote the IA and KA waves. The electron Landau damping is neglected in obtaining (20) and (21). The parallel components of the electric fields associated with the IA and KA waves are, respectively (Shukla and Stenflo 2004)

$$E_z = i\left[\frac{m_e\omega^2(1+b_e)}{b_e e k_z n_0}\right] n_{e1}^{I} \tag{22}$$

and

$$E_z = -i\frac{T_e k_z}{e n_0} n_{e1}^{K}. \tag{23}$$

The wave magnetic field is determined from $\mathbf{B}_\perp = (c/\omega)\mathbf{k}\times\mathbf{E}$. Noting that $\omega \ll \omega_{ci} \ll \omega_{pi}$ for the shear Alfvén waves in a dense plasma, we obtain from (19) the dispersion relations

$$\omega^2 = \frac{k_z^2 V_A^2 b_i}{[1-\Gamma_0(b_i)](1+b_e)}, \tag{24}$$

for the IA waves, and

$$\omega^2 = k_z^2 V_A^2\left[b_s + \frac{b_i}{1-\Gamma_0(b_i)}\right], \tag{25}$$

for the KA waves. For $b_i \ll 1$, we have $\Gamma_0 \approx 1 - b_i + 3b_i^2/4$, so that (24) and (25) give the familiar results for the IA and KA wave frequencies, respectively:

$$\omega = \frac{k_z V_A}{(1+k_\perp^2\lambda_e^2)^{1/2}} \tag{26}$$

and

$$\omega \approx k_z V_A (1+k_\perp^2\rho^2)^{1/2}, \tag{27}$$

where $\rho^2 = \rho_s^2 + 3\rho_i^2/4$. For $k_\perp^2\lambda_e^2 \gg 1$, (24) gives $\omega = k_z(\omega_{ce}\omega_{ci})^{1/2}/k_\perp$, which is the Okuda–Dawson convective cell frequency (Okuda and Dawson 1973). It is obvious that the IA and KA waves appear in plasmas with $\beta \ll m_e/m_i$ and $m_e/m_i \ll \beta \ll 1$, respectively, where $\beta = 8\pi n_0 T/B_0^2$ and $T = T_e + T_i$. The quasi-neutrality approximation also allows us to write the parallel electric fields associated with the IA and KA waves as (Shukla and Stenflo 2004)

$$E_z = \frac{[1-\Gamma_0(b_i)]\omega^2|\mathbf{E}_\perp|}{k_\perp k_z C_a^2} \tag{28}$$

https://doi.org/10.1017/S0022377809990031 Published online by Cambridge University Press

and

$$E_z = \frac{c^2 k_z^3 \lambda_{\rm De}^2 |\mathbf{k}_\perp \cdot \mathbf{E}_\perp|}{\omega^2 - k_z^2 V_{\rm A}^2 b_{\rm s}}, \tag{29}$$

where $C_{\rm a} = (T_{\rm i}/m_{\rm e})^{1/2}$ is the electron acoustic speed. The dispersion relation and the relationship between the parallel and perpendicular electric fields presented above are frequently used to understand the properties of dispersive Alfvén waves in space and laboratory plasmas. Mode conversion of a surface magnetohydrodynamic wave to a kinetic Alfvén wave is a well-known process in plasma physics (Hasegawa and Chen 1976). Here, a surface wave such as a Kelvin–Helmholtz wave mode converts to an Alfvén wave.

4. Ponderomotive force and plasma density modification

In the following, we discuss the ponderomotive force of the DSAWs and the associated plasma density modification. The quasi-stationary plasma slow response in the DSAW fields is given by (Shukla et al. 2004)

$$m_{\rm e}\left(\langle \mathbf{v}_{\rm e\perp} \cdot \nabla v_{\rm ez}\rangle + \frac{1}{2}\langle v_{\rm ez}^2\rangle\right) + \frac{e}{c}\langle (\mathbf{v}_{\rm e\perp} \times \mathbf{B}_\perp)_z\rangle = -eE_z^{\rm s} - T_{\rm e}\partial_z \ln n_{\rm e}^{\rm s}, \tag{30}$$

$$m_{\rm i}\left(\langle \mathbf{v}_{\rm i\perp} \cdot \nabla v_{\rm iz}\rangle + \frac{1}{2}\langle v_{\rm iz}^2\rangle\right) - \frac{e}{c}\langle (\mathbf{v}_{\rm i\perp} \times \mathbf{B}_\perp)_z\rangle = eE_z^{\rm s} - T_{\rm i}\partial_z \ln n_{\rm i}^{\rm s}, \tag{31}$$

where the superscript 's' denotes the quantities associated with the plasma slow motion. The angular bracket denotes averaging over the DSAW period. We first consider the DSAWs with $k_z V_{\rm Te} \ll \omega \ll \omega_{\rm ce}$, so that the appropriate fluid velocities are

$$\mathbf{v}_{\rm e\perp} \approx \frac{c}{B_0}\mathbf{E}_\perp \times \hat{\mathbf{z}}, \quad v_{\rm ez} = -i\frac{eE_z}{m_{\rm e}\omega} \tag{32}$$

and

$$\mathbf{v}_{\rm i\perp} \approx \frac{e\omega_{\rm ci}}{m_{\rm i}(\omega_{\rm ci}^2 - \omega^2)}\mathbf{E}_\perp \times \hat{\mathbf{z}} - i\frac{c\omega\omega_{\rm ci}\mathbf{E}_\perp}{B_0(\omega_{\rm ci}^2 - \omega^2)}. \tag{33}$$

The perpendicular component of the current density is

$$\mathbf{J}_\perp = -\frac{n_0 ec}{B_0}\frac{\omega^2}{\omega_{\rm ci}^2 - \omega^2}\mathbf{E}_\perp \times \hat{\mathbf{z}} - i\frac{n_0 ec\omega\omega_{\rm ci}\mathbf{E}_\perp}{B_0(\omega_{\rm ci}^2 - \omega^2)}, \tag{34}$$

Accordingly, we have a balance between the ponderomotive force and the pressure gradient:

$$\frac{i}{n_0\omega}\langle \mathbf{J}_\perp^* \cdot \nabla E_z\rangle - \frac{1}{n_0 c}\langle (\mathbf{J}_\perp^* \times \mathbf{B}_\perp)\rangle + \frac{e^2}{4m_{\rm e}\omega^2}\frac{\partial}{\partial z}|E_z|^2 = -(T_{\rm e} + T_{\rm i})\frac{\partial}{\partial z}\ln n_{\rm e}^{\rm s}. \tag{35}$$

Here the asterisk denotes the complex conjugate
By using the wave magnetic field

$$\mathbf{B}_\perp = -i\frac{c}{\omega}(\nabla \times \mathbf{E})_\perp \tag{36}$$

as well as the electric field relationship

$$\frac{\omega^2\omega_{\rm ci}}{(\omega_{\rm ci}^2 - \omega^2)\omega_{\rm ce}}\nabla \cdot \mathbf{E}_\perp = \frac{\partial E_z}{\partial z} \tag{37}$$

https://doi.org/10.1017/S0022377809990031 Published online by Cambridge University Press

and the modified IA wave dispersion relation

$$\frac{\omega^2(1+k_\perp^2\lambda_{\rm e}^2)}{k_z^2\lambda_{\rm i}^2}=\omega_{\rm ci}^2-\omega^2, \tag{38}$$

we obtain the quasi-neutral density response (Shukla et al. 2004)

$$n_{\rm e}=n_0\exp\left[\frac{|B_y|^2}{16\pi n_0(T_{\rm e}+T_{\rm i})}\right]. \tag{39}$$

On the other hand, for the modified KAWs we take $v_{ez}=i(e\omega/k_z^2T_{\rm e})E_z$ and obtain (Shukla et al. 2004)

$$n_{\rm e}^{\rm s}=n_0\exp\left[\frac{e^2|\mathbf{E}_\perp|^2}{4m_{\rm i}(T_{\rm e}+T_{\rm i})(\omega_{\rm ci}^2-\omega^2)}-\frac{e^2|E_z|^2}{4m_{\rm e}(T_{\rm e}+T_{\rm i})}\frac{\omega^2}{k_z^4V_{\rm Te}^4}\right]. \tag{40}$$

Since for the modified KAWs we have

$$E_z=\frac{k_zk_\perp C_{\rm s}^2|\mathbf{E}_\perp|}{\omega_{\rm ci}^2-\omega^2}, \tag{41}$$

$$\omega^2=\frac{k_z^2V_{\rm A}^2}{1+k_z^2\lambda_{\rm i}^2}(1+k_\perp^2\rho_{\rm s}^2), \tag{42}$$

the quasi-stationary electron response for the KAWs turns out to be

$$n_{\rm e}^{\rm s}=n_0\exp\left[\frac{\alpha e^2|\mathbf{E}_\perp|^2}{4m_{\rm i}(T_{\rm e}+T_{\rm i})(\omega_{\rm ci}^2-\omega^2)}\right], \tag{43}$$

where $\alpha=1-\omega^2k_\perp^2m_{\rm e}/(\omega_{\rm ci}^2-\omega^2)k_z^2m_{\rm i}$. The expressions (39) and (43) reveal that the ponderomotive force of the DSAWs produces magnetic field-aligned electron density compressions.

5. Modulated circularly polarized dispersive Alfvén waves

Let us now consider the amplitude modulation of circularly polarized dispersive Alfvén waves (CPDAWs) along the external magnetic field direction. The cold plasma dispersion relation for CPDAWs ($\omega\ll\omega_{\rm ce},\mathbf{k}\parallel\hat{\mathbf{z}}$) is

$$\frac{k^2c^2}{\omega^2}\approx\pm\frac{\omega_{\rm pe}^2}{\omega\omega_{\rm ce}}-\frac{\omega_{\rm pi}^2}{\omega(\omega\pm\omega_{\rm ci})}, \tag{44}$$

which for $\omega\sim kV_{\rm A}\ll\omega_{\rm ci}$ reduces to

$$\omega\approx kV_{\rm A}\left(1\mp\frac{kV_{\rm A}}{2\omega_{\rm ci}}\right). \tag{45}$$

Suppose that the nonlinear interaction between CPDAWs and the plasma slow response produces an envelope of waves which varies slowly. Hence, we introduce the eikonal representation (Shukla et al. 2004)

$$\omega\to\omega_0+i\frac{\partial}{\partial t}-iV_{\rm A0}\frac{\partial}{\partial z},\quad k\to k_0-i\frac{\partial}{\partial z} \tag{46}$$

in (45) and operate on the wave electric field $\mathbf{E}=E_\perp(\hat{\mathbf{x}}\pm i\hat{\mathbf{y}})$. Assuming that $\partial E_\perp/\partial t\ll\omega_0E_\perp\equiv\omega_0(E_x\mp iE_y)$, we then obtain the derivative nonlinear

https://doi.org/10.1017/S0022377809990031 Published online by Cambridge University Press

Schrödinger equation (DNLSE)

$$\left(\frac{\partial}{\partial t}+V_{\rm A0}\frac{\partial}{\partial z}\right)E_\perp-\frac{V_{\rm A}}{2n_0}\frac{\partial}{\partial z}(n_1E_\perp)\pm\frac{iV_{\rm A0}^2}{2\omega_{\rm ci}}\frac{\partial^2E_\perp}{\partial z^2}=0. \tag{47}$$

The slow plasma response assumes inertialess electrons:

$$0=-eE^{\rm s}-\frac{T_{\rm e}}{n_0}\frac{\partial n_1}{\partial z}\pm\frac{\omega_{\rm pe}^2}{4\pi n_0\omega\omega_{\rm ce}}\frac{\partial|E_\perp|^2}{\partial z} \tag{48}$$

and inertial ions:

$$m_{\rm i}\frac{\partial v_{\rm i}^{\rm s}}{\partial t}=eE^{\rm s}-\frac{\gamma_{\rm i}T_{\rm i}}{n_0}\frac{\partial n_1}{\partial z}-\frac{\omega_{\rm pi}^2}{4\pi n_0\omega(\omega\pm\omega_{\rm ci})}\frac{\partial|E_\perp|^2}{\partial z}. \tag{49}$$

Eliminating the ambipolar electric field $E^{\rm s}$ from (48) and (49) and using the ion continuity equation, we obtain the driven ion sound waves

$$\left(\frac{\partial^2}{\partial t^2}-C_{\rm s}^2\frac{\partial^2}{\partial z^2}\right)n_1=-\frac{n_0c^2}{B_0^2}\frac{\partial^2|E_\perp|^2}{\partial z^2}. \tag{50}$$

The quasi-stationary response is then

$$\frac{n_1}{n_0}=\frac{m_{\rm i}c^2}{T_{\rm e}+T_{\rm i}}\frac{|E_\perp|^2}{B_0^2}. \tag{51}$$

Subsequently, (47) takes the form (Shukla et al. 2004)

$$\left(\frac{\partial}{\partial t}+V_{\rm A0}\frac{\partial}{\partial z}\right)E_\perp-\frac{m_{\rm i}V_{\rm A0}c^2}{2(T_{\rm e}+T_{\rm i})B_0^2}\frac{\partial}{\partial z}(|E_\perp|^2E_\perp)\pm\frac{iV_{\rm A0}^2}{2\omega_{\rm ci}}\frac{\partial^2E_\perp}{\partial z^2}=0. \tag{52}$$

The DNLSE (52) admits a localized DAW electric field envelope accompanied with a background plasma density compression.

6. Nonlinear interactions between DAWs

Satellite (ICB1300) data (Chmyrev et al. 1988) and recent Cluster observations (Sundkvist et al. 2005) from the magnetospheric cusp region have unambiguously discovered coherent vortices as a manifestation of Alfvénic turbulence. Accordingly, it is desirable to have the knowledge of the governing nonlinear equations, which admit an inverse cascade responsible for the formation of Alfvén vortices. In the following, we present a set of nonlinear equations (Shukla et al. 2004) for nonlinearly interacting low-frequency (in comparison with $\omega_{\rm ci}$), long-wavelength (in comparison with the ion gyroradius) three-dimensional DAWs. For our purposes, the appropriate fluid velocities are then

$$\mathbf{v}_{\rm e\perp}\approx\frac{c}{B_0}\hat{\mathbf{z}}\times\nabla\phi-\frac{c}{eB_0n_{\rm e}}\hat{\mathbf{z}}\times\nabla(n_{\rm e}T_{\rm e})+v_{\rm ez}\frac{\nabla_\perp A_z\times\hat{\mathbf{z}}}{B_0}, \tag{53}$$

$$\mathbf{v}_{\rm i\perp}\approx\frac{c}{B_0}\hat{\mathbf{z}}\times\nabla\phi-\frac{c}{B_0\omega_{\rm ci}}\left(\partial_t+\frac{c}{B_0}\hat{\mathbf{z}}\times\nabla\phi\cdot\nabla\right)\nabla_\perp\phi, \tag{54}$$

$$v_{\rm ez}\approx\frac{c}{4\pi en_0}\nabla_\perp^2A_z. \tag{55}$$

https://doi.org/10.1017/S0022377809990031 Published online by Cambridge University Press

Substituting (53)–(55) into $\nabla \cdot \mathbf{J} = 0$, where $\mathbf{J} = \mathbf{J}_\perp + \hat{\mathbf{z}} J_z$ is the plasma current density, we obtain

$$\frac{d}{dt}\nabla_\perp^2 \phi + \frac{V_A^2}{c}\frac{d}{dz}\nabla_\perp^2 A_z = 0, \tag{56}$$

where $d/dt = (\partial/\partial t) + (c/B_0)\hat{\mathbf{z}} \times \nabla\phi \cdot \nabla$ and $d/dz = (\partial/\partial z) - B_0^{-1}\hat{\mathbf{z}} \times \nabla A_z \cdot \nabla$. For the IAWs, we neglect the parallel electron pressure gradient in the parallel electron momentum equation and obtain

$$\frac{d}{dt}(1 - \lambda_e^2 \nabla_\perp^2) A_z + c\partial_z \phi = 0. \tag{57}$$

On the other hand, for the KAWs the parallel electron inertia is negligible in comparison with the electron pressure gradient. Thus, we have

$$\frac{\partial A_z}{\partial t} + c\frac{d}{dz}\left(\phi - \frac{T_e n_1}{e n_0}\right) = 0, \tag{58}$$

where the electron continuity equation

$$\frac{dn_1}{dt} + \frac{c}{4\pi e}\frac{d}{dz}\nabla_\perp^2 A_z = 0 \tag{59}$$

determines n_1. Equations (56)–(59) are complex nonlinear partial differential equations containing vector nonlinearities. They admit dual cascades and provide the possibility of self organization (Hasegawa 1985) of DAWs in the form of different types of vortical structures (Jovanovic et al. 1998; Petviashvili and Pokhotelov 1992; Shukla et al. 1995) (e.g. dipolar and tripolar vortices and a vortex street). Equations (56)–(59) can also be expressed in Hamiltonian form, and they are useful for studying collisionless tearing modes and current filaments in plasmas with sheared magnetic fields (Del Sarto et al. 2003). Furthermore, in a non-uniform magnetoplasma with the equilibrium density gradient, (56)–(59) have to be modified by including the effects of the density inhomogeneities. In such a situation we will have nonlinearly interacting drift-Alfvén waves (Shukla et al. 1986).

7. Generation of zonal flows by kinetic Alfvén waves

The nonlinear couplings (Sagdeev et al. 1978a,b; Shukla 2005; Shukla et al. 1981) between the dispersive drift and kinetic Alfvén waves and zonal flows/convective cells (Okuda and Dawson 1973) (also referred to as sheared flows) have been a topic of significant interest in space and laboratory plasmas. It is established that sheared flows can inhibit the transport of plasma particles across the external magnetic field direction. In this section, we present a theory for the generation of convective cells. Following Shukla (2005), we use the two-fluid model and account for the combined action of the nonlinear ion polarization drifts and the coupling of the parallel electron flow with the sheared magnetic field of KAWs and the convective cell motions/zonal flows. The electron and ion fluid velocities in the presence of nonlinearly interacting low-frequency ($\ll\omega_{ci}$) DKAWs and zonal flows are, respectively,

$$\mathbf{v}_{e\perp} \approx \frac{c}{B_0}\hat{\mathbf{z}} \times \nabla\phi - \frac{cT_e}{eB_0 n_0}\hat{\mathbf{z}} \times \nabla n_1 \tag{60}$$

https://doi.org/10.1017/S0022377809990031 Published online by Cambridge University Press

and

$$\mathbf{v}_{\mathrm{i}\perp} \approx \frac{c}{B_0}\hat{\mathbf{z}}\times\nabla\phi - \frac{c}{B_0\omega_{\mathrm{ci}}}\left[\left(\frac{\partial}{\partial t}+\nu_{\mathrm{in}}+\mu_{\mathrm{i}}\nabla_\perp^2\right)\nabla_\perp\phi + \frac{c}{B_0}(\hat{\mathbf{z}}\times\nabla\psi\cdot\nabla)\nabla_\perp\phi \right.$$
$$\left. + \frac{c}{B_0}(\hat{\mathbf{z}}\times\nabla\phi\cdot\nabla)\nabla_\perp\psi\right], \tag{61}$$

where ν_{in} is the ion–neutral collision frequency, $\mu_{\mathrm{i}} = 0.3\nu_{\mathrm{ii}}\rho_{\mathrm{i}}^2$ is the coefficient of the ion gyroviscosity, ν_{in} (ν_{ii}) is the ion–neutral (ion–ion) collision frequency, ψ is the potential of zonal flows and $T_{\mathrm{e}} \gg T_{\mathrm{i}}$ has been assumed. The appropriate electron and ion velocities involved in zonal flows in the presence of the DKAWs are, respectively,

$$\mathbf{u}_{\mathrm{e}\perp} \approx \frac{c}{B_0}\hat{\mathbf{z}}\times\nabla\psi + \frac{\langle v_{\mathrm{e}z}\mathbf{B}_\perp\rangle}{B_0} \tag{62}$$

and

$$\mathbf{u}_{\mathrm{i}\perp} \approx \frac{c}{B_0}\hat{\mathbf{z}}\times\nabla\psi - \frac{c}{B_0\omega_{\mathrm{ci}}}\left[\left(\frac{\partial}{\partial t}+\nu_{\mathrm{in}}+\mu_{\mathrm{i}}\nabla_\perp^2\right)\cdot\nabla_\perp\psi + \frac{c}{B_0}\langle(\hat{\mathbf{z}}\times\nabla\phi\cdot\nabla)\nabla_\perp\phi\rangle\right], \tag{63}$$

where the parallel component of the electron fluid velocity in the DKAW fields is

$$v_{\mathrm{e}z} \simeq \frac{c}{4\pi e n_0}\nabla_\perp^2 A_z, \tag{64}$$

which is obtained from the parallel component of Ampère's law, with $\mathbf{B}_\perp = \nabla A_z\times\hat{\mathbf{z}}$. In (64) we have neglected the parallel ion motion, as we are isolating the ion acoustic waves in our intermediate plasma. The last terms on the right-hand sides of (62) and (63) are the Reynolds stresses of the KAWs, which reinforce two-dimensional zonal flows. Substituting (60) and (61) into $\nabla\cdot\mathbf{J} = 0$, where $\mathbf{J} = en_0(\mathbf{v}_{\mathrm{i}\perp} - \mathbf{v}_{\mathrm{e}\perp} - v_{\mathrm{e}z}\hat{\mathbf{z}})$, we have

$$\frac{\partial}{\partial t}\nabla_\perp^2\phi + \frac{V_{\mathrm{A}}^2}{c}\frac{\partial}{\partial z}\nabla_\perp^2 A_z + \frac{c}{B_0}(\hat{\mathbf{z}}\times\nabla\psi\cdot\nabla)\nabla_\perp^2\phi + \frac{c}{B_0}(\hat{\mathbf{z}}\times\nabla\phi\cdot\nabla)\nabla_\perp^2\psi = 0, \tag{65}$$

where we have assumed that $|\partial\phi/\partial t| \gg (\nu_{\mathrm{in}} + \mu_{\mathrm{i}}\nabla_\perp^2)\phi$. The quasi-neutrality condition $n_{\mathrm{e}1} = n_{\mathrm{i}1} = n_1$ holds in a dense plasma with $\omega_{\mathrm{pi}} \gg \omega_{\mathrm{ci}}$, where $\omega_{\mathrm{pi}} = (4\pi n_0 e^2/m_{\mathrm{i}})^{1/2}$ is the ion plasma frequency. From the parallel component of the inertialess electron equation of motion, we obtain

$$\frac{\partial}{\partial t}A_z + c\frac{\partial}{\partial z}\left(\phi - \frac{T_{\mathrm{e}}n_1}{en_0}\right) + \frac{c}{B_0}\hat{\mathbf{z}}\times\nabla\psi\cdot\nabla A_z = 0. \tag{66}$$

On the other hand, the ion continuity equation, together with (63), yields

$$\left(\frac{\partial}{\partial t} + \frac{c}{B_0}\hat{\mathbf{z}}\times\nabla\psi\cdot\nabla\right)\left(n_1 - \frac{cn_0}{B_0\omega_{\mathrm{ci}}}\nabla_\perp^2\phi\right) = 0. \tag{67}$$

The equation for two-dimensional zonal flows is obtained by inserting (64) and (65) into the electron and ion continuity equations, respectively, and substituting them into Poisson's equation. We obtain

$$\left(\frac{\partial}{\partial t} + \nu_{\mathrm{in}} + 0.3\nu_{\mathrm{ii}}\rho_{\mathrm{i}}^2\nabla_\perp^2\right)\nabla_\perp^2\psi + \frac{c}{B_0}\langle(\hat{\mathbf{z}}\times\nabla\phi\cdot\nabla)\nabla_\perp^2\phi\rangle - \frac{V_{\mathrm{A}}^2}{cB_0}\langle(\hat{\mathbf{z}}\times\nabla A_z\cdot\nabla)\nabla_\perp^2 A_z\rangle = 0, \tag{68}$$

where, to lowest order, we must use

$$\frac{\partial A_z}{\partial z} + \frac{c}{V_{\mathrm{A}}^2}\frac{\partial\phi}{\partial t} = 0 \tag{69}$$

https://doi.org/10.1017/S0022377809990031 Published online by Cambridge University Press

in the last term of (68) to eliminate A_z in terms of ϕ. Equations (65)–(68) form a closed system of equations for studying the excitation of zonal flows by finite-amplitude KAWs. In the following, we derive a general dispersion relation for the modulational instability of a constant-amplitude DAW pump against zonal flow perturbations. For this purpose, we decompose the high-frequency potentials into those of the pump and the two sidebands, viz.

$$\phi = \phi_{0+}\exp(-i\omega_0 t + i\mathbf{k}_0\cdot\mathbf{r}) + \phi_{0-}\exp(i\omega_0 t - i\mathbf{k}_0\cdot\mathbf{r}) + \sum_{+,-}\phi_{\pm}\exp(-i\omega_{\pm}t + i\mathbf{k}_{\pm}\cdot\mathbf{r}), \tag{70}$$

$$A_z = A_{z0+}\exp(-i\omega_0 t + i\mathbf{k}_0\cdot\mathbf{r}) + A_{z0-}\exp(i\omega_0 t - i\mathbf{k}_0\cdot\mathbf{r}) + \sum_{+,-}A_{z\pm}\exp(-i\omega_{\pm}t + i\mathbf{k}_{\pm}\cdot\mathbf{r}), \tag{71}$$

where $\omega_{\pm} = \Omega \pm \omega_0$ and $\mathbf{k}_{\pm} = \mathbf{K} \pm \mathbf{k}_0$ are the frequency and wavevector of the upper and lower DAW sidebands. The subscripts $0_{\pm}$ and $\pm$ represent the pump and sidebands, respectively. Assuming further that $\psi = \varphi\exp(-i\Omega t + i\mathbf{K}\cdot\mathbf{r})$, we insert (70) and (71) into (65)–(67), Fourier transform them and combine the resultant equations to obtain

$$D_{\pm}\phi_{\pm} = \pm\frac{ic}{B_0}\hat{\mathbf{z}}\times\mathbf{k}_0\cdot\mathbf{K}\left(\omega_0 + \omega_{\pm}\frac{k_{0\perp}^2 - k_{\perp}^2}{k_{\perp\pm}^2}\right)\varphi\phi_{0\pm}, \tag{72}$$

where $D_{\pm} = \omega_{\pm}^2 - k_{z0}^2V_{\rm A}^2(1+k_{\perp\pm}^2\rho_{\rm s}^2) \approx \pm 2\omega_0(\Omega - \mathbf{K}_{\perp}\cdot\mathbf{V}_{{\rm g}\perp}) \mp \delta$, with $\omega_0 = k_{z0}V_{\rm A}(1+k_{\perp 0}^2\rho_{\rm s}^2)^{1/2}$, $\mathbf{V}_{{\rm g}\perp} = \mathbf{k}_{0\perp}\rho_{\rm s}^2k_{z0}^2V_{\rm A}^2/\omega_0$ and $\delta = k_{z0}^2V_{\rm A}^2k_{\perp}^2\rho_{\rm s}^2/2\omega_0$. On the other hand, inserting (70) and (71) into (68) and Fourier transforming the resultant equation, we have

$$(\Omega + i\Gamma_z)\varphi = i\frac{2c}{B_0}\frac{\hat{\mathbf{z}}\times\mathbf{k}_0\cdot\mathbf{K}}{k_{\perp}^2}\left(1 - \frac{\omega_0^2}{k_{z0}^2V_{\rm A}^2}\right)(\mathscr{K}_-^2\phi_{0+}\phi_- - \mathscr{K}_+^2\phi_{0-}\phi_+), \tag{73}$$

where $\Gamma_z = \nu_{\rm in} + 0.3\nu_{\rm ii}k_{\perp}^2\rho_{\rm i}^2$ and $\mathscr{K}_{\pm}^2 = k_{\perp\pm}^2 - k_0^2 \equiv k_{\perp}^2 \pm 2\mathbf{k}_{0\perp}\cdot\mathbf{K}_{\perp}$. Equation (73) reveals that the coupling constant on the right-hand side remains finite only if $\omega_0 \neq k_{0z}V_{\rm A}$. Thus, dispersion to Alfvén waves is required in order for the parametric coupling between convective cells and the KAWs to remain intact. Eliminating $\phi_{\pm}$ from (73) by using (72), we finally obtain the nonlinear dispersion relation

$$\Omega + i\Gamma_z = \frac{2c^2\omega_0|\phi_0|^2}{B_0^2}\frac{|\hat{\mathbf{z}}\times\mathbf{k}_0\cdot\mathbf{K}|^2}{k_{\perp}^2}k_{0\perp}^2\rho_{\rm s}^2\sum_{+,-}\frac{\mathscr{K}_{\pm}^2\kappa_{\pm}^2}{k_{\perp\pm}^2D_{\pm}}, \tag{74}$$

where $\kappa_{\pm}^2 = k_{\perp}^2 \pm \mathbf{k}_{0\perp}\cdot\mathbf{K}_{\perp}$. We see from (15) that the coupling constant on the right-hand side is proportional to $k_{0\perp}^2\rho_{\rm s}^2$, which is a feature of the kinetic Alfvén wave dispersion. For long-wavelength zonal flows with $|\mathbf{K}_{\perp}| \ll |\mathbf{k}_{0\perp}|$, (74) reduces to

$$(\Omega + i\Gamma_z)[(\Omega - \mathbf{K}_{\perp}\cdot\mathbf{V}_{{\rm g}\perp})^2 - \delta^2] = -2k_{\perp}^2c^2\delta\frac{|E_{0\perp}|^2}{B_0^2}k_{0\perp}^2\rho_{\rm s}^2|(\hat{\mathbf{K}}\cdot\hat{\mathbf{k}}_{0\perp})(\hat{\mathbf{z}}\times\hat{\mathbf{k}}_0\cdot\hat{\mathbf{K}})|^2, \tag{75}$$

where $|E_{0\perp}|^2 = k_{0\perp}^2|\phi_0|^2$ and $\hat{\mathbf{K}}_{\perp}$ and $\hat{\mathbf{k}}_{0\perp}$ are the unit vectors. We analyze (75) in two limiting cases. First, we let $\Omega = \mathbf{K}_{\perp}\cdot\mathbf{V}_{{\rm g}\perp} + i\gamma_{\rm m}$ in (75) and obtain for

https://doi.org/10.1017/S0022377809990031 Published online by Cambridge University Press

$\gamma_{\rm m}, \Gamma_z \ll |\mathbf{K}_\perp \cdot \mathbf{V}_{g\perp}|$ the growth rate

$$\gamma_{\rm m} = \left[\frac{2k_\perp^2 c^2 k_{0\perp}^2 \rho_{\rm s}^2 \delta}{|\mathbf{K}_\perp \cdot \mathbf{V}_{g\perp}|} \frac{|E_{0\perp}|^2}{B_0^2} \times |(\hat{\mathbf{K}} \cdot \hat{\mathbf{k}}_{0\perp})(\hat{\mathbf{z}} \times \hat{\mathbf{k}}_0 \cdot \hat{\mathbf{K}})|^2 - \delta^2 \right]^{1/2}. \tag{76}$$

The expression (76) shows that the modulational instability sets in if

$$|E_{0\perp}|^2 > \frac{B_0^2 \delta |\mathbf{K}_\perp \cdot \mathbf{V}_{g\perp}|}{2k_\perp^2 c^2 k_{0\perp}^2 \rho_{\rm s}^2 |(\hat{\mathbf{K}} \cdot \hat{\mathbf{k}}_{0\perp})(\hat{\mathbf{z}} \times \hat{\mathbf{k}}_0 \cdot \hat{\mathbf{K}})|^2}. \tag{77}$$

Second, for $\Omega \gg \Gamma_z, \mathbf{K}_\perp \cdot \mathbf{V}_{g\perp}, \delta$, we have from (75)

$$\Omega^3 \simeq -2k_\perp^2 c^2 \delta \frac{|E_{0\perp}|^2}{B_0^2} k_{0\perp}^2 \rho_{\rm s}^2, \tag{78}$$

which admits a reactive instability whose growth rate is

$$\gamma_{\rm r} \approx (K_\perp c)^{2/3} \delta^{1/3} (k_{0\perp}\rho_{\rm s})^{2/3} \left(\frac{|E_{0\perp}|}{B_0} \right)^{2/3}. \tag{79}$$

We observe from (79) that the increment is proportional to the two-thirds power of $k_{0\perp}\rho_{\rm s}$ and the KAW pump electric field strength $|E_{0\perp}|$. For plasmas with $n_0 = 2 \times 10^{12}$ cm^{-3}, $B_0 = 1.5$ kG and $T_{\rm e} = 10T_{\rm i} = 10$ eV, we have $\beta m_{\rm i}/m_{\rm e} \approx 30$, $V_{\rm A} = 10^8$ cm/s and $\rho_{\rm s} = 0.25$ cm. Taking $k_{0\perp}\rho_{\rm s} = 0.1$, $\omega_0 \sim 10^5$ s^{-5}, $K_\perp/k_{0\perp} \sim 0.1$ and $|E_{0\perp}| \sim 10^{-4} B_0$, we find that $\delta \sim 10$ s^{-1}, $|\mathbf{K}_\perp \cdot \mathbf{V}_{\rm g}| \sim 100$ s^{-1} and $\gamma_{\rm r} \sim 10^3$ s^{-1}. Thus, the reactive instability can produce zonal flows within a millisecond at the expense of the kinetic Alfvén wave energy. It is expected that zonal flows driven by the dispersive kinetic Alfvén waves can play a significant role in regulating the transport of plasma particles in magnetoplasmas, such as those in the Large Plasma Device (LAPD) at the University of California Los Angeles (UCLA) (Carter et al. 2006; Gekelman 1999), as well as in the Earth's magnetosphere and in the solar corona.

8. The electron Joule heating by high-frequency DAWs

It has been known (Hasegawa and Chen 1976; Hasegawa and Uberoi 1982) for some time that the dispersive kinetic Alfvén waves can cause heating of the plasma particles in laboratory plasmas. The idea of wave–particle interactions (Hasegawa and Chen 1976) has been utilized to understand the solar coronal electron heating, which is an outstanding central problem in solar physics (Edwin and Murawski 1995; Harrison 1997; Kellett and Tsikoudi 1997; Klimchuck 2006; Laing and Edwin 1995; Narain and Ulmschneider 1996; Tsiklauri 2006). About 10 years ago, Shukla et al. 1999 proposed that the solar coronal electron heating could be caused by the resonant interaction between the high-frequency electromagnetic ion-cyclotron-Alfvén (HF-EMICA) waves, which have a magnetic field-aligned electric field. The latter facilitates the electron Joule heating due to the wave–electron interaction, as described below. Let us present the essential mathematical steps that are required for understanding the origin of the electron Joule heating. We note that the HF-EMICA waves are mixed modes with a magnetic field-aligned electric field component, and consequently there are density perturbations associated with the HF-EMICA waves. The dispersion relation of low parallel phase velocity (in comparison with the electron thermal speed) long-wavelength (in comparison with the ion

https://doi.org/10.1017/S0022377809990031 Published online by Cambridge University Press

gyroradius) DA waves in a collisionless plasma is (Shukla et al. 1999, 2006)

$$\omega = \frac{\omega_{\rm A}}{(1+k_z^2\lambda_{\rm i}^2)^{1/2}}\left[1+\left(\frac{3}{4}+\frac{T_{\rm e}}{T_{\rm i}}\right)k_x^2\rho_{\rm i}^2\right]^{1/2}, \tag{80}$$

where the wave frequency ω is much smaller than the electron gyrofrequency $\omega_{\rm ce} = eB_0/m_{\rm e}c$, and k_x is the component of the wavevector across the ambient magnetic field direction. In obtaining (84), we have neglected the parallel ion dynamics, as the parallel phase speed of the EMICA waves is much larger than the ion sound speed. We note that the parallel dispersive term (the $\lambda_{\rm i}$ term) in (80) arises from the perpendicular ion inertial force, whereas the term involving 3/4 comes from the ion finite Larmor radius effect, and the term involving $T_{\rm e}/T_{\rm i}$ comes from the parallel electron kinetics. In a plasma with $T_{\rm e} \gg T_{\rm i}$, the perpendicular dispersion solely arises from the parallel electron pressure gradient force, and the square bracket in (80) is replaced by $1 + k_x^2\rho_{\rm s}^2$, where $\rho_{\rm s} = c_{\rm s}/\omega_{\rm ci}$ is the ion sound gyroradius and $c_{\rm s} = (T_{\rm e}/m_{\rm i})^{1/2}$ the ion acoustic speed. When the parallel wavelength is shorter than the ion skin depth, (80) gives $\omega \approx \omega_{\rm ci}(1 + k_x^2\rho_{\rm s}^2)^{1/2}$, which is the frequency of ion cyclotron waves in a plasma with $T_{\rm e} \gg T_{\rm i}$. In the following, we shall present the parallel electron current density associated with the HF-EMICA waves, and discuss the associated electron heating rate arising from the dissipation of the perturbed electron current density. By using the linearized drift kinetic equation (Hasegawa and Mima 1978) for the perturbed electron distribution function, we obtain an expression for the parallel (to **z**) electron current density J_{ez} in a Maxwellian plasma. The result is (Bellan 1998)

$$J_{ez} = i\frac{\omega E_z}{8\pi k_z^2\lambda_{\rm De}^2}Z'(\xi_{\rm e}), \tag{81}$$

where E_z is the parallel electric field, $\lambda_{\rm De} = (T_{\rm e}/4\pi n_0 e^2)^{1/2}$ the electron Debye radius and Z' the derivative of the standard plasma dispersion function with argument $\xi_{\rm e} = \omega/\sqrt{2}k_z V_{\rm te}$. Here, $V_{\rm te} = (T_{\rm e}/m_{\rm e})^{1/2}$ is the electron thermal speed. For $\xi_{\rm e} \ll 1$, (81) becomes

$$J_{ez} = -i\frac{\omega E_z}{4\pi k_z^2\lambda_{\rm De}^2}[1 + i\sqrt{\pi}\xi_{\rm e}\exp(-\xi_{\rm e}^2)]. \tag{82}$$

The electron heating rate in the collisionless regime is governed by the dissipation of the magnetic field-aligned electron current, viz. (Shukla et al. 1999c, 2006)

$$\frac{dT_{\rm e}}{dt} = \frac{1}{2n_0}{\rm Re}(J_{ez}E_z^*) \equiv \sqrt{\pi}\frac{\omega_{\rm ci}^2\omega_{\rm pe}^2|E_z|^2(1+b_{\rm s})}{4\pi n_0 k_z^3 v_{\rm te}^3(1+b_{\rm i})}, \tag{83}$$

where $b_{\rm s} = k_x^2\rho_{\rm s}^2(1 + 3T_{\rm i}/4T_{\rm e})$, $b_{\rm i} = k_z^2\lambda_{\rm i}^2$, $\omega_{\rm pe} = (4\pi n_0 e^2/m_{\rm e})^{1/2}$ and the asterisk stands for the complex conjugate. Equation (83) exhibits that the electrons are rapidly heated by intense localized parallel electric fields of the HF-EMICA waves. The localization of the parallel electric field is caused by the self modulation (Mikhailovskii et al. 1977; Shukla et al. 1998) of the HF-EMICA wave packets by non-resonant density perturbations. We now apply the results of our theoretical model to the electron heating in the solar corona: accordingly, we use some typical plasma and field parameters that are appropriate for the coronal heating scenario. The electron number density and the electron temperature in the unperturbed state are typically 5×10^9 cm^{-3} and 1 million K, respectively, whereas the ambient magnetic field is of the order of 10 G. Thus, we have $\omega_{\rm pe} = 4 \times 10^9$ rad s^{-1},

https://doi.org/10.1017/S0022377809990031 Published online by Cambridge University Press

$\omega_{ci} = 10^5$ rad s^{-1}, $V_{te} = 4 \times 10^8$ cm s^{-1}, $V_A = 3 \times 10^7$ cm s^{-1}, $c_s = (T_e/m_i)^{1/2} = 10^7$ cm s^{-1} and $\beta = 8\pi n_0 T/B_0^2 = 0.2$. The ion Larmor radius is roughly $\rho_s \approx 1$ m and the ion skin depth (λ_i) turns out to be 3 m. Assuming that both the perpendicular and parallel wavelengths of the DA waves are 1 m, we have $k_x \rho_s \approx 6$ and $k_z \lambda_i = 18$. It then follows from (83) that within 5–10 s the electron temperature will rise to a value of 5 million K when the parallel electric field of the DA waves is 0.5 V cm^{-1}. For our adopted nominal value of the parallel electric field (0.5 V cm^{-1}), we find that $E_z/B_0 = 1.6 \times 10^{-5}$. Thus, the electron–HF-EMICA wave interactions are capable of producing the desired electron heating in the solar corona. The heating rate is sufficiently rapid to balance the cooling losses by conduction or radiation.

9. Ion heating by magnetic field-aligned EMICA waves

In the past, many authors (Chen et al. 2001; McChesney et al. 1987; White et al. 2002) have discussed stochastic ion heating in the electrostatic and electromagnetic fields that have electric fields perpendicular to the external magnetic field direction. In the following, we consider differential ion heating in the solar corona caused by magnetic field-aligned left-hand circularly polarized EMICA waves that seem to have been observed (Cranmer 2001; Cranmer et al. 1999; Li 2002) indirectly. The wave magnetic field is of the form

$$\mathbf{B}_w = \sum_k B_k (\hat{\mathbf{x}} - i\hat{\mathbf{y}}) \exp(-i\omega_k t + ikz + i\varphi_k) + \text{c.c.}, \tag{84}$$

where $\hat{\mathbf{x}}$ and $\hat{\mathbf{y}}$ are the unit vectors along the x and y axes, respectively, $\omega_k = (k^2 c^2 \omega_{ci}/2\omega_{pi}^2)(\sqrt{1 + 4\omega_{pi}^2/k^2 c^2} - 1)$ is the EMICA wave frequency, $k \equiv k_z$, φ_k is the phase constant and c.c. stands for the complex conjugate. In (84) the wave magnetic field is a resultant vector field composed of a large number of discrete components with different wavenumbers. The ions in the EMICA wave fields obey the equation of motion

$$\frac{d\mathbf{v}}{dT} = \frac{e}{m_i}\left[\mathbf{E}_w + \frac{\mathbf{v}}{c} \times (\hat{\mathbf{z}} B_0 + \mathbf{B}_w)\right], \tag{85}$$

where $\mathbf{v} = d\mathbf{r}/dt$ is the ion velocity. The wave electric field $\mathbf{E}$ is obtained from

$$\hat{\mathbf{z}} \times \mathbf{E}_w = \frac{\omega_k}{kc} \mathbf{B}_w. \tag{86}$$

From (85) and (86), we then obtain (Shukla et al. 2006)

$$\frac{dv_x}{dt} = \frac{e}{m_i c} \sum_k \left(\frac{\omega_k}{k} - v_z\right) B_{ky} \exp(i\phi_k) + \omega_{ci} v_y, \tag{87}$$

$$\frac{dv_y}{dt} = -\frac{e}{m_i c} \sum_k \left(\frac{\omega_k}{k} - v_z\right) B_{kx} \exp(-i\phi_k) - \omega_{ci} v_x \tag{88}$$

and

$$\frac{dv_z}{dt} = \frac{e}{m_i c} \sum_k (v_x B_{ky} - v_y B_{kx}) \exp(-i\phi_k), \tag{89}$$

https://doi.org/10.1017/S0022377809990031 Published online by Cambridge University Press

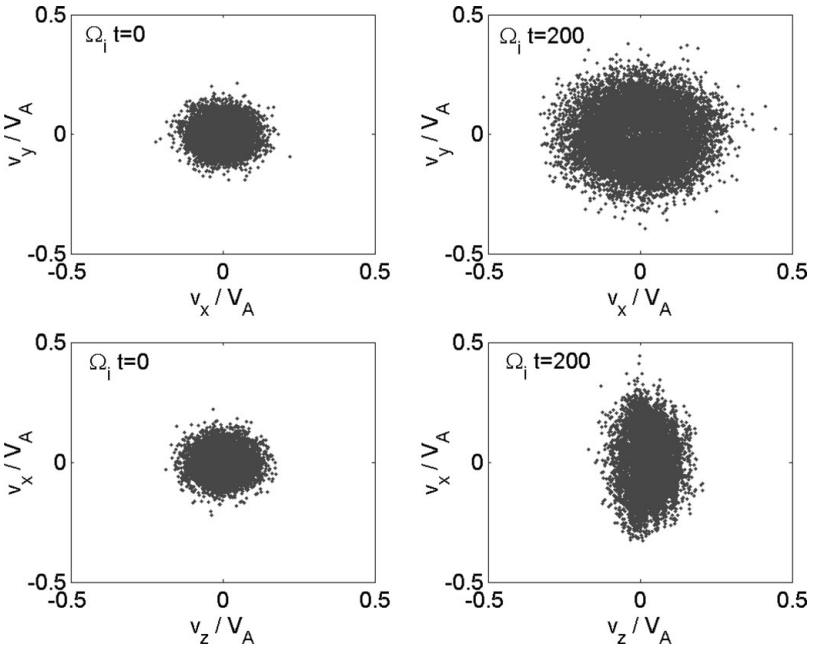


Figure 1. The ion particle distribution at $t = 0$ (left-hand panels) and $\omega_{ci}t = 200$ (right-hand panels) in the v_x–v_y plane (upper panels) and in the v_z–v_x plane (lower panels). The initially isotropic distribution (left-hand panels) becomes strongly anisotropic due to differential heating of the ions in the perpendicular direction by EMICA waves. After Shukla et al. (2006).

where we have denoted $\mathbf{v} = (v_x, v_y, v_z)$, $\mathbf{B}_w = (B_{kx}, B_{ky}, 0)$ and $\phi_k = \omega_k t - kz - \varphi_k$. For left-hand circularly polarized EMICA waves, we introduce $u_\perp = v_x - iv_y$ and $B_{k\perp} = B_{kx} - iB_{ky}$ to obtain from (87)–(89)

$$\frac{du_\perp}{dt} - i\omega_{ci}u_\perp = -i\sum_k \left(v_z - \frac{\omega_k}{k}\right)\Omega_k \exp(-i\phi_k) \tag{90}$$

and

$$\frac{dv_z}{dt} = \mathrm{Im}[u_\perp \Omega_k^* \exp(i\phi_k)], \tag{91}$$

where $\Omega_k = (e/m_i c)(B_{kx} - iB_{ky})$ is the gyrofrequency associated with the wave magnetic field. We have numerically solved (Shukla et al. 2006) (90) and (91) to demonstrate the ion energization in the magnetic field-aligned EMICA wave magnetic fields. In the simulation, we used 10 randomly phased waves, each of amplitude $|\Omega_k| = 0.01\,\omega_{ci}$ and with equally spaced frequencies between $\omega_k = 0.6\omega_{ci}$ and $\omega_k = 1.5\omega_{ci}$. The simulation was performed with 10^4 test particles with initial conditions $u_\perp = u_\perp(0)$, $v_z = v_z(0)$ and $z = z(0)$ that were Maxwellian distributed with an isotropic temperature corresponding to an ion thermal speed of $0.05\,V_A$ in all velocity directions. Figure 1 shows the initial and isotropic ion distribution at time $t = 0$ and the particle distribution at $t = 200\,\omega_{ci}$, where the latter is strongly non-isotropic. The ion heating has been taking place in the perpendicular direction only while the thermal spread in the parallel z direction is the same as at $t = 0$. This differential ion heating is demonstrated in Fig. 2, where we have

https://doi.org/10.1017/S0022377809990031 Published online by Cambridge University Press

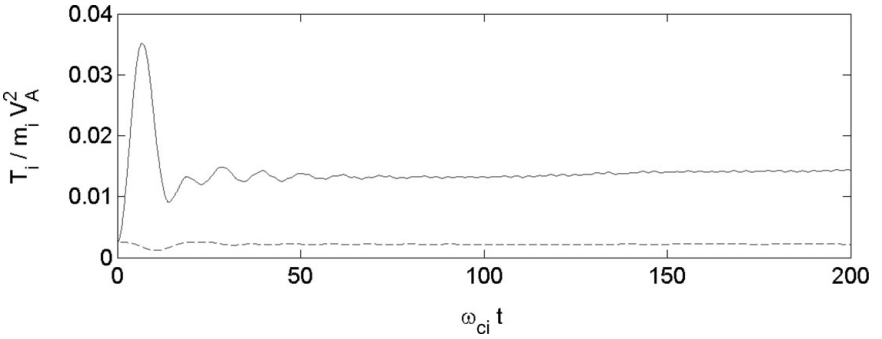


Figure 2. The perpendicular (solid line) and parallel (dashed line) ion temperatures as a function of time. The initially isotropic temperature becomes strongly anisotropic due to differential stochastic heating by nonlinear EMICA waves. At $\omega_{ci}t = 200$, the temperature ratio is approximately $T_\perp/T_z = 5$. After Shukla et al. (2006).

displayed the parallel and perpendicular ion temperatures as a function of time. We see that the ion temperature, which initially is isotropic, is enhanced strongly in the perpendicular direction only. After some time, the ion temperatures stabilize with a temperature ratio $T_\perp/T_z \approx 5$. This is in agreement with the observed ion temperature anisotropy in the solar corona (Gary et al. 2005). It should be stressed that the test-particle approach used in this section is not self consistent, since the electromagnetic field is given as an external input and not calculated from the Maxwell equations. Hence, we have not taken into account the damping of the wave via the heating process. Such effects may be important and should be studied in more realistic, self-consistent studies of the wave–ion interactions.

10. Solar coronal heating by lower-hybrid drift modes

A key ingredient of the heating process is photospheric convection that slowly creates an interwoven random magnetic field topology. For weak fields the plasma particles would dominate, creating currents to prevent the build up of interwoven magnetic structures; the result would be a loss of low-temperature plasma forming a slow solar wind. For strong fields, however, confinement and convective cells in the photosphere combine to form interwoven magnetic fields creating tangential discontinuities (i.e. current sheets). X-ray bright points or blinkers (Harrison 1997) are seen bubbling on the surface and associated with cancellation of opposing magnetic flux indicating the formation of current sheets. These current sheets give rise to plasma micro-instabilities resulting in plasma heating. The current sheet separating regions of opposing field lines can be responsible for a number of instabilities. One of the fastest-growing instabilities driven by the cross-field current is the lower-hybrid instability. Another instability responsible for generating lower-hybrid waves is from ions reflected at shocks such as the slow shock in reconnection. The reflected ions form a cross-field flow resulting in the excitation of lower-hybrid waves through the modified two-stream instability. Lower-hybrid drift modes can be easily generated at plasma boundaries where density and magnetic field gradients exist. It is well known from the study of laboratory plasmas and magnetospheric plasmas that these waves play a role in plasma stability and transport (Trines et al. 2005, 2007).

https://doi.org/10.1017/S0022377809990031 Published online by Cambridge University Press

Both lower-hybrid and lower-hybrid drift modes are unstable at some threshold value to strong turbulence effects leading to wave collapse and caviton formation within which both electrons and ions can be energized (Bingham et al. 2001). The lower-hybrid drift waves can resonate with both slow-moving ions perpendicular to the magnetic field and relatively energetic electrons moving parallel to the magnetic field. Lower-hybrid waves can also be generated by ion horseshoe distributions (Bingham et al. 2002, 1999). The waves provide an effective means of transferring energy between the ions and electrons providing a means of energizing electrons to high energies. Strong turbulence effects such as wave collapse can also play a role in energizing electrons. The linear stage leading to strong turbulence is the modulational instability, which results in wave collapse and the formation of filamentary density cavities with lower-hybrid wave packets trapped inside. This process creates cascading to shorter wavelengths leading to Landau resonance at $\omega = k_\perp V_{\rm Ti}$ with unmagnetized ions and at $\omega = k_\parallel v_{\rm e\parallel}$ with magnetized electrons. A theory of electron acceleration by lower-hybrid turbulence, using marginal stability arguments, will be presented. Marginal stability analysis yields energies and scale lengths appropriate to solar current sheets. We assume that the lower-hybrid drift instability is operating in the kinetic regime $v_{\rm oi} \ll V_{\rm Ti}$. Its maximum growth rate is

$$\gamma = \frac{\sqrt{2\pi}}{8}\left(\frac{v_{\rm Di}}{V_{\rm Ti}}\right)^2 \omega_{\rm lh}, \tag{92}$$

with a perpendicular wavenumber of

$$k_{\rm m} = \sqrt{2}\frac{\omega_{\rm lh}}{V_{\rm Ti}} = \sqrt{2}\left(\frac{m_{\rm e}}{m_{\rm i}}\right)^{1/2}\frac{\Omega_{\rm ce}}{V_{\rm Ti}}, \tag{93}$$

where

$$\frac{v_{\rm Di}}{V_{\rm Ti}} = \frac{1}{2}\left(\frac{r_{\rm Li}}{\Delta x_\perp}\right) \tag{94}$$

and

$$\Delta x_\perp^{-1} = \frac{\partial \ln \rho}{\partial x_\perp} \approx \frac{\partial \ln B}{\partial x_\perp}. \tag{95}$$

The rate at which lower-hybrid waves (LHWs) is damped is obtained by assuming that the waves Landau damp on electrons moving parallel to the magnetic field and ions moving perpendicular to the field. Demanding that the waves have time to grow places a constraint on the damping rate; we require that

$$\gamma_{\rm D} \approx 10\frac{v_\perp}{\Delta x_\perp}. \tag{96}$$

Equating (92) and (96) yields the characteristic scale length required to maintain the drift current at marginal stability. We find that

$$\Delta x_\perp \approx \frac{1}{5}\frac{\sqrt{2\pi}}{32} r_{\rm Li}\sqrt{\frac{m_{\rm i}}{m_{\rm e}}} \approx r_{\rm Li} \tag{97}$$

for $v_\perp \sim V_{\rm Ti}$. If we now demand a balance between the Poynting flux of electromagnetic energy flowing into the tail and the rate of ohmic dissipation, we find the resistivity required:

$$\eta = \frac{4\pi u \Delta x_\perp}{c^2}. \tag{98}$$

https://doi.org/10.1017/S0022377809990031 Published online by Cambridge University Press

Now, $\eta = 4\pi\nu_\perp/\omega_{\rm pe}^2$, which implies that

$$\nu_\perp = \frac{4\pi}{\omega_{\rm pe}^2}\frac{4\pi u \Delta x_\perp}{c^2} = \omega_{\rm pe}\frac{\omega_{\rm pe}}{c}\frac{u}{c}\Delta x_\perp$$

but

$$\nu_\perp = \omega_{\rm pe}\frac{\langle \delta E^2\rangle}{8\pi nkT}$$

or

$$\frac{\langle \delta E^2\rangle}{8\pi nkT} = \frac{1}{5}\frac{\sqrt{2\pi}}{32}\sqrt{\frac{m_{\rm i}}{m_{\rm e}}}\frac{r_{\rm Li}}{\lambda_{\rm pe}}\frac{u}{c}, \tag{99}$$

where we have used (97) and $\lambda_{\rm pe} = c/\omega_{\rm pe}$ is the plasma skin depth. For nanoflares the parameters we use are $B \approx 200$ G, $n \approx 10^{10}$ cm^{-3}, $\lambda_{\rm De} \simeq 0.2$ cm, $r_{\rm Li} \approx 3$–20 cm, $V_{\rm Ti} \approx 3 \times 10^7$ cm/s and $v_{\rm A} \approx 2.00 \times 10^8$ cm/s. Taking $u \approx 0.1\ v_{\rm A}$, we find that

$$\frac{\langle \delta E^2\rangle}{8\pi nkT} \approx 2.13 \times 10^{-4}.$$

With (98) we can compute the energies and fluxes of non-thermal electrons. An estimate of the change in temperature of the electrons due to the ohmic heating can be obtained by noting that as the plasma flows through and out of the region of instability electrons will experience ohmic heating for a time $\Delta t \approx \Delta x_\parallel/V_{\rm A}$; hence, the change in electron temperature during this period is

$$\Delta k_{\rm B}T \approx \frac{\eta J^2}{n}\frac{\Delta x_\parallel}{V_{\rm A}}$$

or, on using (97) and (98),

$$\Delta k_{\rm B}T \approx \frac{160}{n\sqrt{2\pi}}\sqrt{\frac{m_{\rm e}}{m_{\rm i}}}\frac{u}{v_{\rm A}}\frac{B^2}{4\pi}\frac{\Delta x_\parallel}{r_{\rm Li}}.$$

Using the previous parameters, we find that

$$\Delta T({\rm eV}) \approx 2.9 \times 10^1 \frac{\Delta x_\parallel}{r_{\rm Li}}.$$

For $r_{\rm Li} \approx 5$ cm, $v_{\rm A} \approx 1.37 \times 10^7$ cm/s and $\Delta x_\parallel \approx 3$–$5 r_{\rm Li}$, using

$$\Delta T({\rm eV}) \approx 2.9 \times 10^1 \frac{\Delta x_\parallel}{r_{\rm Li}} \tag{100}$$

results in electron temperatures of the order of a hundred eV or more depending on the extent of the current sheet. The small spatial value chosen reflects the role of the reconnection process taking place. The lower-hybrid drift wave instability (LHDI) also leads to strong ion heating perpendicular to the magnetic field. Equipartition of energy indicates that 2/3 of the available free energy ends up in ion heating and 1/3 ends up in heating the electrons parallel to the magnetic field. The simple calculation below confirms this argument. To estimate the ion temperature, we utilize the fact that the ratio of ion and electron drifts given by

$$\frac{v_{\rm Di}}{v_{\rm De}} = \frac{T_{\rm i}}{T_{\rm e}}$$

https://doi.org/10.1017/S0022377809990031 Published online by Cambridge University Press

together with Ampère's equation yields

$$T_{\rm i} = T_{\rm e}\left(1 + 2\frac{v_{\rm A}}{u}\frac{\Delta x_\perp}{\Delta x_\parallel}\right). \tag{101}$$

To estimate the non-thermal energies of the electrons and their fluxes, we follow a standard approach used by previous authors (Bingham et al. 1991, 1984a,b, 2001; Lampe and Papadopoulos 1977; Spicer et al. 1981). Following Bingham et al. (1991) specifically, we find that the characteristic energy gained by the electrons with finite $k_\parallel$ is

$$\mathscr{E}_{\rm e} \approx \left[\left(\frac{\omega_{\rm pe}}{\Omega_{\rm ce}}\right)^2 \frac{\langle \delta E^2\rangle}{4\pi n} m_{\rm e} v_{\rm A}^2 \omega_{\rm lh} \Delta x_\parallel \sqrt{m_{\rm e}}\right]^{2/5}$$

or

$$\mathscr{E}_{\rm e} \approx \left[\frac{\omega_{\rm pe}^2}{\Omega_{\rm ce}} \frac{\langle \delta E^2\rangle}{4\pi n k T_{\rm e}} C_{\rm s}^2 m_{\rm i} m_{\rm e} v_{\rm A}^2 \left(\frac{m_{\rm e}}{m_{\rm i}}\right)^{1/2} \Delta x_\parallel \sqrt{m_{\rm e}}\right]^{2/5}, \tag{102}$$

where $c_{\rm s}^2 = k_{\rm B} T_{\rm e}/m_{\rm i}$ is the ion acoustic speed. To estimate the number density $n_{\rm T}$ of particles that are stochastically accelerated, we take as the initial distribution a Maxwellian distribution and integrate it from $\varepsilon V_{\rm Te}$ to infinity to yield

$$\frac{n_{\rm T}}{n} \approx \frac{1}{\sqrt{\pi}} \frac{e^{-\epsilon^2}}{\epsilon}, \tag{103}$$

where ϵ is the smallest number of thermal speeds we expect the LHW with finite $k_\parallel$ to resonantly interact with. Since $k_\parallel \approx (m_{\rm e}/m_{\rm i})^{1/2} k_\perp$ for maximum growth and $k_\perp \approx \sqrt{2}(m_{\rm e}/m_{\rm i})^{1/2}\Omega_{\rm ce}/V_{\rm Ti}$, we have $v_{\rm p}^{\rm min} \approx 2.3\, v_{\rm Te}$ so that $n_{\rm T}/n \approx 10^{-3}$.

11. Discussion and conclusion

In this paper, we have presented the underlying physics and the dispersion properties of dispersive shear Alfvén waves (DSAWs) in a uniform magnetoplasma. We have obtained a general dispersion relation that includes the finite $\omega/k_z V_{\rm Te}$ and the finite $\omega/\omega_{\rm ci}$ effects, in addition to the finite ion Larmor radius and electron skin depth corrections. It is shown that these non-ideal effects drastically modify the propagation characteristics of the DSAWs in plasmas. Large-amplitude DSAWs are shown to produce local plasma density enhancement due to the ponderomotive force. The latter is also responsible for creating non-resonant density perturbations which modulate the magnetic field-aligned dispersive Alfvén waves. The modulated dispersive Alfvén wave packets along the magnetic field direction obey a DNLSE, which admits localized wave envelopes. The dynamics of nonlinearly interacting three-dimensional dispersive Alfvén waves is governed by a set of equations in which the ion vorticity, the ion number density perturbation and the parallel component of the vector potential are related in a complex manner. Since the governing nonlinear equations contain the vector nonlinearities, they admit a dual cascade, which ensures the formation of Alfvén vortices. The latter were recently observed in space plasmas. Furthermore, we have presented a nonlinear theory for the generation of sheared plasma flows by the Reynolds stresses of the kinetic Alfvén waves. The presence of sheared plasma flows provides the possibility of a better plasma confinement in magnetically confined fusion plasmas. We have also discussed the nonlinear aspects of EMICA waves, which are responsible for the

https://doi.org/10.1017/S0022377809990031 Published online by Cambridge University Press

heating of plasma particles in the solar corona. Attention is paid to electron Joule heating by the obliquely propagating HF-EMICA waves and ion heating by magnetic field-aligned left-hand circularly polarized EMICA waves. Both mechanisms involve wave–particle interactions and are capable of yielding the desired electron heating and ion temperature anisotropy in the solar corona that are consistent with observations. It should be noted that there is some indirect evidence (Cranmer et al. 1999, Cranmer 2001; Li 2002) for the existence of the HF-EMICA and left-hand circularly polarized EMICA waves in the solar corona. These waves could be excited due to the ion temperature anisotropy (Gary et al. 2005), fast magnetic reconnections (McKenzie et al. 1995), pre-existing ion and electron beams, sheared plasma flows, etc. We stress that the results presented here are useful for understanding the salient features of dispersive Alfvén waves and some important nonlinear effects (associated with wave–wave and wave–particle interactions) that they produce in the Earth's ionosphere and magnetosphere, in the solar corona and in LAPD at UCLA (Carter et al. 2006). We have presented possible wave–particle heating processes that can produce the required temperature in the solar corona. We have discussed the possibility of the electron heating in the solar corona by high-frequency dispersive kinetic Alfvén waves, which have a magnetic field-aligned electric field. Physically, the heating arises from the dissipation of the parallel electron current due to the electron Landau damping. On the other hand, the ion heating caused by the HFDKAWs is insignificant in low-β collisionless corona plasmas. The present investigation can easily be generalized by including the streaming of multi-ion components in the solar corona. However, we believe that the inclusion of the multi-ion species will somewhat modify the HFDKAW spectrum, but the essential physics of the electron heating due to wave–particle interactions would remain intact. In conclusion, we stress that the present mechanism of wave–particle interactions is very important for a localized heating of electrons by the HFDKAWs which have a parallel electric field. In the collisionless solar coronal plasma, the electron heating based on the resistive MHD description is not practical and efficient, as there one has to introduce an anomalous resistivity in an ad hoc manner. We have also demonstrated that the lower-hybrid drift wave instability can generate relatively large amplitude lower-hybrid waves in current sheets. These lower-hybrid waves are shown to be capable of accelerating electrons and heating ions during the reconnection process. The process describes the microphysics of particle heating. The present mechanism is important where magnetic reconnection is invoked to explain particle heating and acceleration in the solar corona. In all cases non-Maxwellian distribution functions arise, which may be possible to determine from spectral analysis.

Acknowledgements

This work was partially supported by the Centre for Fundamental Physics (CfFP) at Rutherford Appleton Laboratory, Chilton (UK), as well as by the Deutsche Forschungsgemeinschaft (Bonn) through the project SH21/3-1 of the Research Unit 1048, and the Swedish Research Council. RB would like to thank N. Legge for assistance in preparing the paper.

References

[1] Alfvén, H. 1942 *Nature* **150**, 405.
[2] Bellan, P. M. 1998 *Phys. Plasmas* **5**, 3081.

https://doi.org/10.1017/S0022377809990031 Published online by Cambridge University Press

[3] Bingham, R., Bryant, D. A. and Hall, D. S. 1984a *Geophys. Res. Lett.* **11**, 327.
[4] Bingham, R., Bryant, D. A. and Hall, D. S. 1984b *Ann. Geophys.* **6**, 159.
[5] Bingham, R., Shapiro, V. D., Tsytovich, V. N., de Angelis, U., Gilman, M. and Shevchenko, V. I. 1991 *Phys. Fluids* B **63**, 1729.
[6] Bingham, R., Cairns, R. A., Dendy, R. O., Shapiro, V. D., Shukla, P. K. and Stenflo, L. 2001 *Phys. Chem. Earth (c)*, **26**, 133.
[7] Bingham, R., Dawson, J. and Shapiro, V. D. 2002 *J. Plasma. Phys.* **68**, 161.
[8] Brambilla, M. 1988 *Kinetic Theory of Plasma Waves: Homogeneous Plasmas*. Oxford: Clarendon.
[9] Brodin, G. and Stenflo, L. 1990 *Contrib. Plasma Phys.* **30**, 413.
[10] Carter, T. A., Brugman, R., Pribyl, P. and Lybarger, W. 2006 *Phys. Rev. Lett.* **96**, 155001.
[11] Champeaux, G. A. et al. 1997 *Astrophys. J.* **486**, 477.
[12] Chen, L., Lin, Z. and White, R. 2001 *Phys. Plasmas* **8**, 4731.
[13] Chmyrev, V. M., Bilichenko, S. V., Pokhotelov, O. A., Marchenko, V. A., Lazarev, V. I., Streltsov, A. V. and Stenflo, L. 1988 *Phys. Scripta* **38**, 841.
[14] Cranmer, S. R., Field, G. B. and Kohl, J. L. 1999 *Astrophys. J.* **518**, 937.
[15] Cranmer, S. R. 2001 *J. Geophys. Res.* **106**(A11), 24937.
[16] Diamond, P. H. and Malkov, M. A. 2006 *Astrophys. J.* **654**, 252.
[17] Drozdenko, T. and Morales, G. J. 2001 *Phys. Plasmas* **8**, 3265.
[18] Edwin, P. M. and Murawski, K. 1995 *Sol. Phys.* **158**, 227.
[19] Feldman, U. and Landi, E. 2008 *Plasma Phys.* **15**, 056501.
[20] Gekelman, W. 1999 *J. Geophys. Res.* **104**, 14417.
[21] Gary, S. P., Skoug, R. M. and Smith, C. W. 2005 *Plasma Phys.* **12**, 056501.
[22] Harrison, R. A. 1997 *Sol. Phys.* **175**, 467.
[23] Hasegawa, A. and Chen, L. 1976 *Phys. Fluids* **19**, 1924.
[24] Hasegawa, A. and Mima, K. 1978 *J. Geophys. Res.* **83**, 1117.
[25] Hasegawa, A. and Uberoi, C. 1982 The Alfvén wave. DOE/TIC Rep. No. 11197, Technical Center, US Department of Energy, Washington, DC.
[26] Hasegawa, A. 1985 *Adv. Phys.* **34**, 1.
[27] Jovanovic, D., Pegoraro, F. and Rasmussen, J. J. 1998 *J. Plasma Phys.* **60**, 383.
[28] Kellett, B. J. and Tsikoudi, V. 1997 *Mon. Not. R. Astron. Soc.* **288**, 411.
[29] Kletzing, C. A. et al. 2003 *Phys. Rev. Lett.* **90**, 035004.
[30] Klimchuck, J. A. 2006 *Sol. Phys.* **234**, 41.
[31] Laing, G. B. and Edwin, P. M. 1995 *Sol. Phys.* **161**, 269.
[32] Lampe, M. and Papadopoulos, K. 1977 *Appl. Phys. J.* **212**, 886, 977.
[33] Li, X. 2002 *Astrophys. J.* **571**, L67.
[34] McChesney, J. M., Stern, R. A. and Bellan, P. M. 1987 *Phys. Rev. Lett.* **59**, 1436.
[35] McKenzie, J. E., Banaszkiewicz, M. and Axford, W. I. 1995 *Astron. Astrophys.* **303**, L45.
[36] Mikhailovskii, A. B., Petviashvili, V. I. and Friedman, A. M. 1977 *JETP Lett.* **24**, 43.
[37] Narain, U. and Ulmschneider, P. 1996 *Space Sci. Rev.* **75**, 453.
[38] Okuda, H. and Dawson, J. M. 1973 *Phys. Fluids* **16**, 408.
[39] Petviashvili, V. I. and Pokhotelov, O. A. 1992 *Solitary Waves in Plasmas and in the Atmosphere*. London: Gordon and Breach.
[40] Sagdeev, R. Z., Shapiro, V. D. and Shevchenko, V. I. 1978a *Sov. J. Plasma Phys.* **4**, 306.
[41] Sagdeev, R. Z., Shapiro, V. D. and Shevchenko, V. I. 1978b *JETP Lett.* **27**, 340.
[42] Sarto Del, D., Califano, F. and Pegoraro, F. 2003 *Phys. Rev. Lett.* **91**, 235001.
[43] Shukla, P. K. 1978 *Nature (Lond.)* **278**, 874.
[44] Shukla, P. K., Yu, M. Y., Rahman, H. U. and Spatschek, K. H. 1981 *Phys. Rev.* A **23**, 312.
[45] Shukla, P. K. and Dawson, J. M. 1984 *Astrophys. J.* **276**, L49.
[46] Shukla, P. K. and Stenflo, L. 1985 *Phys. Fluids* **28**, 1576.

https://doi.org/10.1017/S0022377809990031 Published online by Cambridge University Press

[47] Shukla, P. K., Yu, M. Y. and Stenflo, L. 1986 *Phys. Rev.* A **34**, 3478.
[48] Shukla, P. K. and Stenflo, L. 1995 *Phys. Scripta* **T60**, 32.
[49] Shukla, P. K., Birk, G. T. and Bingham, R. 1995 *Geophys. Res. Lett.* **22**, 671.
[50] Shukla, P. K., Bingham, R. and Dendy, R. O. 1998 *Phys. Lett.* A **239**, 369.
[51] Shukla, P. K. and Stenflo, L. 1999a *Nonlinear MHD Waves and Turbulence* (ed. T. Passot and P. L. Sulem). Berlin: Springer, pp. 1–30.
[52] Shukla, P. K. and Stenflo, L. 1999b *Phys. Plasmas* **6**, 4120.
[53] Shukla, P. K., Stenflo, L. and Bingham, R. 1999 *Phys. Plasmas* **6**, 1677.
[54] Shukla, P. K., Bingham, R., McKenzie, J. F. and Axford, W. I. 1999 *Sol. Phys.* **186**, 61.
[55] Shukla, P. K. and Stenflo, L. 2000a *J. Plasma Phys.* **64**, 125.
[56] Shukla, P. K. and Stenflo, L. 2000b *Phys. Plasmas* **7**, 2738.
[57] Shukla, P. K. and Stenflo, L. 2000c *Phys. Rev. Lett.* **85**, 2408.
[58] Shukla, P. K. and Stenflo, L. 2004 *Geophys. Res. Lett.* **31**, L03810
[59] Shukla, P. K., Stenflo, L., Bingham, R. and Eliasson, B. 2004 *Plasma Phys. Control. Fusion* **46**, B349.
[60] Shukla, P. K. 2005 *Phys. Plasmas* **12**, 012310.
[61] Shukla, P. K., Bingham, R., Eliasson, B., Dieckmann, M. and Stenflo, L. 2006 *Plasma Phys. Control. Fusion* **48**, B249.
[62] Spicer, D. S., Benz, A. O. and Huba, J. D. 1981 *Astron. Astrophys.* **105**, 221.
[63] Stasiewicz, K., Bellan, P., Chaston, C. et al. 2000 *Space Sci. Rev.* **92**, 423.
[64] Stefant, R. J. 1971 *Phys. Fluids* **13**, 440.
[65] Sundkvist, D., Krasnoselskikh, V., Shukla, P. K. et al. 2005 *Nature (Lond.)* **436**, 825.
[66] Trines, R., Bingham, R., Silva, L. O., Mendonca, J. T., Shukla, P. K. and Mori, W. B. 2005 *Phys. Rev. Lett.* **94**, 1650021.
[67] Trines, R., Bingham, R., Silva, L. O., Mendonca, J. T. and Shukla, P. K. 2007 *Phys. Rev. Lett.* **99**, 205006.
[68] Tsiklauri, D. 2006 *New. J. Phys.* **8**, 79 43.
[69] White, R., Chen, L. and Lin, Z. 2002 *Phys. Plasmas* **9**, 1890.
[70] Whitlam, S., Ashbourne, J. M. A., Bingham, R., Shukla, P. K. and Spicer, D. S. 2002 *Sol. Phys.* **211**, 199.

https://doi.org/10.1017/S0022377809990031 Published online by Cambridge University Press